Protein Science (1999), *8*:1445–1454. Cambridge University Press. Printed in the USA.

Conformational changes in the NS3 protease from hepatitis C virus strain Bk monitored by limited proteolysis and mass spectrometry

STEFANIA ORRÙ,[1,2] FABRIZIO DAL PIAZ,[1] ANNARITA CASBARRA,[1] GABRIELLA BIASIOL,[2] RAFFAELE DE FRANCESCO,[2] CHRISTIAN STEINKÜHLER,[2] AND PIERO PUCCI[1,3]

[1]Centro Internazionale di Servizi di Spettrometria di Massa, CNR-Università di Napoli Federico II, via Pansini 5, 80131 Napoli, Italy
[2]Department of Biochemistry, Istituto di Ricerche di Biologia Molecolare "P. Angeletti" (IRBM), Via Pontina Km 30,600, 00040 Pomezia, Italy
[3]Dipartimento di Chimica Organica e Biologica, Università di Napoli Federico II, Napoli, Italy

(RECEIVED November 2, 1998; ACCEPTED March 27, 1999)

Abstract

Conformational changes occurring within the NS3 protease domain from the hepatitis C virus Bk strain ($NS3_{1–180}$) under different physico-chemical conditions either in the absence or in the presence of its cofactor Pep4A were investigated by limited proteolysis experiments. Because the surface accessibility of the protein is affected by conformational changes, when comparative experiments were carried out on $NS3_{1–180}$ either at different glycerol concentrations or in the presence of Pep4A, differential peptide maps were obtained from which protein regions involved in the structural changes could be inferred. The surface topology of isolated $NS3_{1–180}$ in solution was essentially consistent with the crystal structure of the protein with the N-terminal segment showing a high conformational flexibility. At higher glycerol concentration, the protease assumed a more compact structure showing a decrease in the accessibility of the N-terminal segment that either was forced to interact with the protein or originate intermolecular interactions with neighboring molecules. Binding of the cofactor Pep4A caused the displacement of the N-terminal arm from the protein moiety, leading this segment to again adopt an open and flexible conformation, thus suggesting that the N-terminus of the protease contributes only marginally to the stability of the complex. The observed conformational changes might be directly correlated with the activation mechanism of the protease by either the cosolvent or the cofactor peptide because they lead to tighter packing of the substrate binding site.

Keywords: conformational analysis; hepatitis C virus; limited proteolysis; mass spectrometry; NS3 protease; selective chemical modifications

Hepatitis C virus (HCV), the major agent causing posttransfusional non-A, non-B hepatitis (Houghton et al., 1991), contains a single positive-strand RNA genome that encodes for a single polyprotein of about 3,000 amino acids (Kato et al., 1990; Choo et al., 1991; Takamizawa et al., 1991). The mature viral proteins are generated by the proteolytic action of both host and viral proteases. Among the latter, the N-terminal domain of NS3 protein contains a chymotrypsin-like protease responsible for four out of five cleavage events taking place during the maturation of the nonstructural (NS) region of the polyprotein (Bartenschlager et al., 1993; Eckart et al., 1993; Grakoui et al., 1993; Hijikata et al., 1993; Tomei et al., 1993; Komoda et al., 1994). NS3 is a 630 amino acid protein that, in addition to the protease domain, contains an RNA helicase domain encompassing the C-terminal two-third of the molecule; however, the helicase portion is not required for optimum protease activity (Failla et al., 1995). The NS3 protease domain was expressed in heterologous systems, purified, and characterized, and used for both structural and functional studies (Shoji et al., 1995; Suzuki et al., 1995; Butkiewicz et al., 1996; Mori et al., 1996; Steinkühler et al., 1996a).

In vivo, NS3 performs its proteolytic functions upon interacting with the viral polypeptide cofactor NS4A, a 54-residue protein that binds the N-terminal region of NS3 through a central hydrophobic segment spanning residues 21–34 (Failla et al., 1994, 1995; Lin

Reprint requests to: Professor Piero Pucci, Centro Internazionale di Servizi di Spettrometria di Massa, CNR-Università di Napoli Federico II, via Pansini 5, 80131 Napoli, Italy; e-mail: pucci@unina.it.

Abbreviations: CD, circular dichroism; CHAPS, 3-(3-cholamidopropyl) dimethylammonio-1-propane sulfonate; DTT, dithiothreitol; ESMS, electrospray mass spectrometry; ER, endoplasmic reticulum; HCV, hepatitis C virus; NS, nonstructural; RP-HPLC, reverse-phase high-performance liquid chromatography, TFA, trifluoroacetic acid.

et al., 1994; Bartenschlager et al., 1995; Tanji et al., 1995; Satoh et al., 1995). Formation of the NS3/NS4A complex greatly enhances proteolytic cleavages at all sites being an absolute requirement for in vivo processing at the NS4B/NS5A junction (Failla et al., 1994). Recently, kinetic and spectroscopic studies showed that formation of the complex between the NS3 protease domain and a peptide encompassing the central hydrophobic domain of NS4A, Pep4A, is sufficient to elicit full activation of the protease (Lin et al., 1995; Butkiewicz et al., 1996; Koch et al., 1996; Steinkühler et al., 1996a; Tomei et al., 1996; Bianchi et al., 1997; Urbani et al., 1997).

The crystal structure of the free protease domain (Love et al., 1996) and of the enzyme complexed to NS4A-derived peptides (Kim et al., 1996; Yan et al., 1998) revealed many details of the interactions occurring in the complex. However, a number of peculiar features of the NS3 protease remain to be fully clarified. The crystal structure of the free protease, obtained in the presence of low concentrations of glycerol, showed an unexpected open conformation of the active site where the catalytic triad is not properly aligned. In the three-dimensional structure of the complex, the N-terminus of NS3 makes extensive contacts with the cofactor peptide, giving rise to tight interactions. However, spectroscopic findings led to the calculation of micromolar equilibrium dissociation constants indicative of a relatively loose complex and poorly compatible with the tight structure observed by X-ray analysis (Bianchi et al., 1997). The concentration of the cosolvent glycerol needed to stabilize the purified protease was shown to have multiple effects on the properties of NS3. The proteolytic activity of NS3 increased with the increase of glycerol concentration, reaching a plateau value at 50% glycerol (Steinkühler et al., 1996b). Similarly, glycerol greatly affected the near-UV region of the CD spectrum of isolated NS3, producing an overall increase in the intensity of the signal that had been interpreted in terms of enhancement of tertiary structure of the protein (Bianchi et al., 1997). Finally, high concentrations of the cosolvent are needed to stabilize the NS3/Pep4A complex, and the binding of the cofactor peptide also increases the activity of the protease (Urbani et al., 1997). Therefore, it is conceivable that, under different physico-chemical conditions, NS3 undergoes structural changes that lead the enzyme to assume its proper biologically active conformation. Information on the structural changes occurring in NS3 in solution is clearly of great importance to define the actual active conformation of the protease, an absolute requirement for the design of appropriate inhibitors.

The aim of this paper is to provide a structural description of the conformational changes responsible for the variations of the enzymatic activity and the spectroscopic properties of the NS3 protease. This investigation has been performed by employing a new strategy that combines limited proteolysis and selective chemical modification experiments with mass spectrometric methodologies. This procedure was developed to probe the surface topology of proteins and to investigate interface regions in protein complexes (Suckau et al., 1992; Glocker et al., 1994; Cohen et al., 1995; Zappacosta et al., 1996, 1997; Scaloni et al., 1998). The conformational changes taking place within the NS3 tertiary structure have been analyzed under different physico-chemical conditions either in the presence or in the absence of its cofactor Pep4A. The results reported here show that, in both cases, the NS3 protease undergoes conspicuous structural changes that mainly affect the extreme N- and C-terminal segments of the molecule with a minor although detectable effect on the active site region.

Results

The proteolytic domain encompassing the N-terminal 181 residues of the NS3 protease from HCV strain BK was cloned and expressed in *Escherichia coli*. To increase protein solubility, a hydrophilic tail containing the sequence Ala-Ser-Lys-Lys-Lys-Lys was added to the C-terminus, producing a 187-amino acid form of the protease ($NS3_{1–180}$) (Steinkühler et al., 1998). The recombinant protein was stable for several hours in a phosphate buffer solution (50 mM) at pH 7.5 containing 10% glycerol, 0.5% 3[(3-cholamidinopropyl) dimethyl ammonium]-1-propane sulfonate (CHAPS), and variable concentrations of DTT in the 0.5–2.5 mM range.

The engineered protein was analyzed by HPLC and characterized by ESMS displaying a molecular mass of 19,538.9 ± 1.5 Da corresponding to a truncated form of the protease lacking the N-terminal Met-Ala dipeptide (Fig. 1). The truncated protease showed biological and spectroscopic properties indistinguishable from intact NS3 and was then used in all the subsequent experiments.

Topological studies of $NS3_{1–180}$

The surface topology of $NS3_{1–180}$ was probed by a combined approach that integrates selective alkylation of cysteine residues, limited proteolysis, and mass spectrometric procedures (Zappacosta et al., 1996, 1997). $NS3_{1–180}$ was reacted with iodoacetamide at pH 7.5, at 25 °C for 10 min in the presence of 2 mM DTT and 10% glycerol. Special care was needed to define the optimum reagent to substrate ratio (0.9:1.0 mol/mol) because the reaction mixture contained a large excess of DTT. The reaction was quenched by lowering the pH to about 2 with 0.1% trifluoroacetic acid (TFA), and the modified species were fractionated by HPLC (Fig. 2). Individual fractions were collected and identified by ESMS analysis. The major component showed a molecular mass of 19,653.1 ± 1.1 Da corresponding to $NS3_{1–180}$ modified by two carboxyamidomethyl groups, whereas the minor species showed the occurrence of a single alkylated Cys residue (measured molecular mass = 19,596.6 ± 1.3 Da). It should be emphasized that both modified forms of $NS3_{1–180}$ may consist of a population of isomers carrying the same number of alkylated residues but located at different sites (Zappacosta et al., 1997).

To identify the modified cysteines, the di-alkylated component was digested with trypsin, and the resulting peptide mixture was fractionated by HPLC. Individual fractions were identified by ESMS leading to the verification of nearly the entire protein structure. The mass values 1,360.1 ± 0.3 and 676.2 ± 0.1 Da could not be assigned to any fragment within the NS3 sequence and were eventually attributed to peptides 13–25 and 157–162, respectively, modified by a single carboxyamidomethyl group. As both fragments contain a single cysteine residue, the modification sites were directly assessed as Cys17 and Cys160. No further modified peptides were detected. These data demonstrated that the major alkylated form of $NS3_{1–180}$ consists of a homogeneous species containing two alkylated cysteine residues. This can be explained in terms of a much higher reactivity of Cys17 and Cys160 compared to the remaining five cysteines, possibly due either to their exposure on the protein surface, or to their chemical microenvironment, or both.

Because the NS3 protease domain is stabilized in the presence of 10% glycerol and DTT, the enzymatic activity of various proteases was evaluated under these experimental conditions prior to

```
                    5                   10                  15                  20
Met-Ala-Pro-Ile-Thr-Ala-Tyr-Ser-Gln-Gln-Thr-Arg-Gly-Leu-Leu-Gly-Cys*-Ile-Ile-Thr

                   25                  30                  35                  40
Ser-Leu-Thr-Gly-Arg-Asp-Lys-Asn-Gln-Val-Glu-Gly-Glu-Val-Gln-Val-Val-Ser-Thr-Ala

                   45                  50                  55                  60
Thr-Gln-Ser-Phe-Leu-Ala-Thr-Cys-Val-Asn-Gly-Val-Cys-Trp-Thr-Val-Tyr-His-Gly-Ala

                   65                  70                  75                  80
Gly-Ser-Lys-Thr-Leu-Ala-Gly-Pro-Lys-Gly-Pro-Ile-Thr-Gln-Met-Tyr-Thr-Asn-Val-Asp

                   85                  90                  95                  100
Gln-Asp-Leu-Val-Gly-Trp-Gln-Ala-Pro-Pro-Gly-Ala-Arg-Ser-Leu-Thr-Pro-Cys-Thr-Cys

                  105                 110                 115                 120
Gly-Ser-Ser-Asp-Leu-Tyr-Leu-Val-Thr-Arg-His-Ala-Asp-Val-Ile-Pro-Val-Arg-Arg-Arg

                  125                 130                 135                 140
Gly-Asp-Ser-Arg-Gly-Ser-Leu-Leu-Ser-Pro-Arg-Pro-Val-Ser-Tyr-Leu-Lys-Gly-Ser-Ser

                  145                 150                 155                 160
Gly-Gly-Pro-Leu-Leu-Cys-Pro-Ser-Gly-His-Ala-Val-Gly-Ile-Phe-Arg-Ala-Ala-Val-Cys*

                  165                 170                 175                 180
Thr-Arg-Gly-Val-Ala-Lys-Ala-Val-Asp-Phe-Val-Pro-Val-Glu-Ser-Met-Glu-Thr-Thr-Met

                  185
Arg-Ala-Ser-Lys-Lys-Lys-Lys
```

Fig. 1. Amino acid sequence of $NS3_{1–180}$. The hydrophilic tail added to the C-terminus is underlined. Primary and secondary preferential cleavage sites are in bold, protease sensitive sites are doubly underlined; the two alkylated cysteines are marked by an asterisk.

limited proteolysis analyses. Preliminary proteolytic experiments showed that elastase, V-8 protease, and endoprotease Asp-N displayed only a very low proteolytic activity under these conditions and, hence, were not used. Limited proteolysis experiments were performed using trypsin, chymotrypsin, subtilisin, and proteinase K as proteolytic probes according to the strategy previously described (Zappacosta et al., 1996; Scaloni et al., 1998). $NS3_{1–180}$ was incubated with each protease using an appropriate enzyme-to-substrate ratio, and the extent of the enzymatic hydrolysis was monitored on a time-course basis by sampling the incubation mixture at different interval times followed by HPLC fractionation. The fragments released from the protein were identified by ESMS leading to the assignment of cleavage sites.

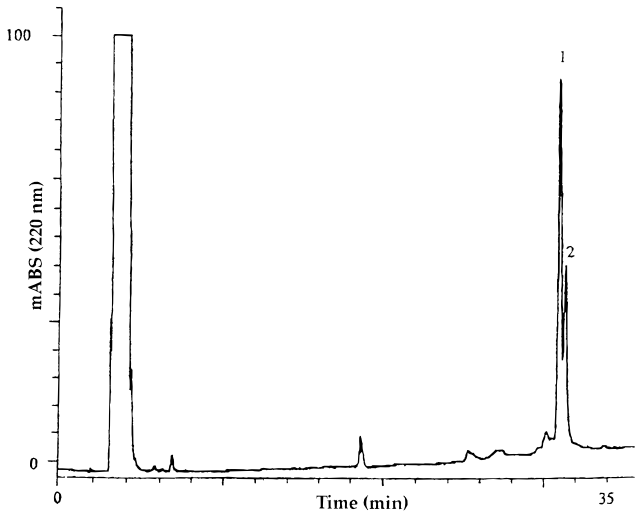

Fig. 2. RP-HPLC profile of $NS3_{1–180}$ modified by iodoacetamide showing the presence of two components.

As an example, Figure 3 shows the HPLC chromatograms of the aliquots withdrawn following 5, 15, and 30 min of chymotrypsin digestion. Protein $NS3_{1–180}$ was immediately cleaved at Tyr7 releasing fragments 3–7 and 8–187 (peaks 2 and 10 in Fig. 3A, respectively). Peak 9 was identified as the peptide 23–187, indicating the occurrence of a secondary cleavage site at Leu22; this interpretation was confirmed by the small fraction 8 containing the fragment 8–22, which clearly originated from the larger peptide 8–187. At later stages of hydrolysis fragments, 8–187 and 23–187 became comparable. Moreover, a series of smaller fragments tend to accumulate essentially with the same kinetics (fractions 1, 3, 4, 5, 6, and 7 in Fig. 3C). Peaks were identified as fragments 129–135, 77–86, 66–76, 87–106, 156–187, and 136–155, respectively, from which protease-sensitive sites could be recognized at Leu65, Tyr76, Trp86, Tyr106, Leu128, Tyr135, and Phe155. Mass spectral identification of the chymotryptic peptides observed within all the proteolysis experiments carried out throughout the paper are reported in Table 1. Peak numbering is consistent within all the chymotryptic digestions (Figs. 3–5).

The overall data from the limited proteolysis experiments are summarized in Table 2 and Figure 1. Preferential cleavage sites were classified as “primary,” “secondary,” and “protease-sensitive” sites merely on qualitative kinetic evaluation according to their

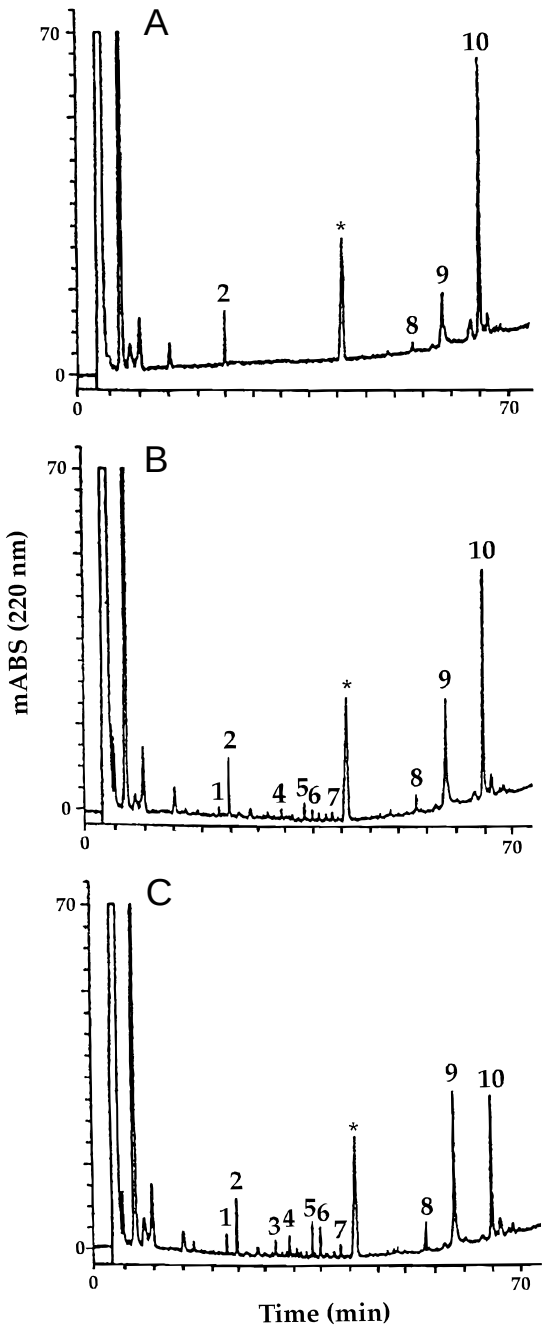

Fig. 3. Time-course analysis of $NS3_{1–180}$ digested with chymotrypsin, at pH 7.5, 25 °C, using an enzyme:substrate ratio of 1:100. HPLC chromatograms of the aliquots withdrawn from the incubation mixture at (**A**) 15 min, (**B**) 30 min, and (**C**) 1 h. Individual fractions were collected and analyzed by ESMS. Peak numbering is consistent within all the chymotryptic digestion experiments (see Figs. 4, 5; Table 1). The CHAPS peak is marked with an asterisk.

rate of appearance and accumulation during the time-course experiments. All the primary and secondary sites are located within the N-terminal segment 7–25, indicating that this region is particularly flexible and exposed. Protease-sensitive sites gathered into two separate regions of the protein, the segment 65–86 and the C-terminal portion from residue 124–179. Few isolated cleavage sites were detected at Arg93, Tyr106, Thr109, and Arg110.

Table 1. *Peptides released from $NS3_{1–180}$ following chymotryptic proteolysis experiments*

Fractions[a]	Peptide	Measured mass	Expected mass
1	129–135	804.5 ± 0.1	804.9
2	3–7	563.4 ± 0.1	563.6
4	66–76	1,161.8 ± 0.3	1,162.4
5	87–106	2,022.7 ± 0.5	2,023.2
6	156–187	3,495.8 ± 0.3	3,496.1
7	136–155	1,896.4 ± 0.6	1,897.2
8	8–22	1,588.9 ± 0.2	1,588.4
9	23–187	17,421.8 ± 0.9	17,421.9
10	8–187	18,992.4 ± 1.1	18,993.8
11	161–180	2,161.7 ± 0.4	2,162.1
12	23–180	16,596.2 ± 1.4	16,596.8
13	8–180	18,167.3 ± 1.0	18,166.8
14	3–187	19,540.3 ± 1.2	19,539.4
15	3–180	18,713.9 ± 1.3	18,715.1

[a] Fractions numbering is consistent within the HPLC profiles shown in Figures 3–5.

Chymotryptic hydrolysis at Phe155 was quite unexpected and deserves some considerations. This residue is located within the hydrophobic pocket forming the NS3 active site, and it is responsible for the specificity of the protease toward small residues (Cys, Thr) (Pizzi et al., 1994). The accessibility of this residue to chymotrypsin suggests that under these conditions the active site of $NS3_{1–180}$ is endowed with considerable conformational flexibility.

Conformational changes of $NS3_{1–180}$ at increasing glycerol concentration

Conformational changes occurring within the $NS3_{1–180}$ structure at different glycerol concentrations were monitored by employing the same limited proteolysis-mass spectrometry approach. Comparative experiments were carried out on the protein in the presence of 10, 25, and 50% glycerol using chymotrypsin as proteolytic probe.

Before incubation with $NS3_{1–180}$, the enzymatic activity of chymotrypsin was evaluated at different glycerol concentrations using the synthetic substrate Suc-Ala-Ala-Pro-Phe-4NA (data not shown).

Table 2. *Preferential cleavage sites detected on the isolated $NS3_{1–180}$ protease*[a]

Protease	Primary sites	Secondary sites	Protease-sensitive sites
Trypsin	Arg12	Arg25	Arg93, Arg110, Arg124, Arg156, Lys166
Chymotrypsin	Tyr7	Leu22	Leu65, Tyr76, Trp86, Tyr106, Leu128, Tyr135, Phe155
Subtilisin	Tyr7	Thr20	Met75, Trp86, Thr109, Val168, Met176, Thr179
Proteinase K	Tyr7	Thr20	Met75, Asn78, Thr109, Arg110, Val152, Val168

[a] Different sites were classified as primary, secondary, and protease-sensitive merely on qualitative kinetic evaluation.

The decrease of proteolytic activity observed at a higher percentage of glycerol was taken into account by increasing the enzyme-to-substrate ratio in the corresponding experiments. $NS3_{1–180}$ was incubated with chymotrypsin in the presence of 10, 25, and 50% glycerol using E/S ratios of 1:100, 1:85, and 1:25, respectively, and the extent of proteolysis was monitored on a time-course basis following the procedure described above.

Figure 4 shows the HPLC profiles corresponding to the 30 min aliquots of the three experiments, and the identification of the individual fractions is reported in Table 1. The data obtained at 10% glycerol (Fig. 4A) essentially confirmed previous results in that Tyr7 and Leu22 were the most accessible sites, with a number of other residues located both in the N- and C-terminal regions of the protein being sensitive to the protease (for a comparison, see Table 2).

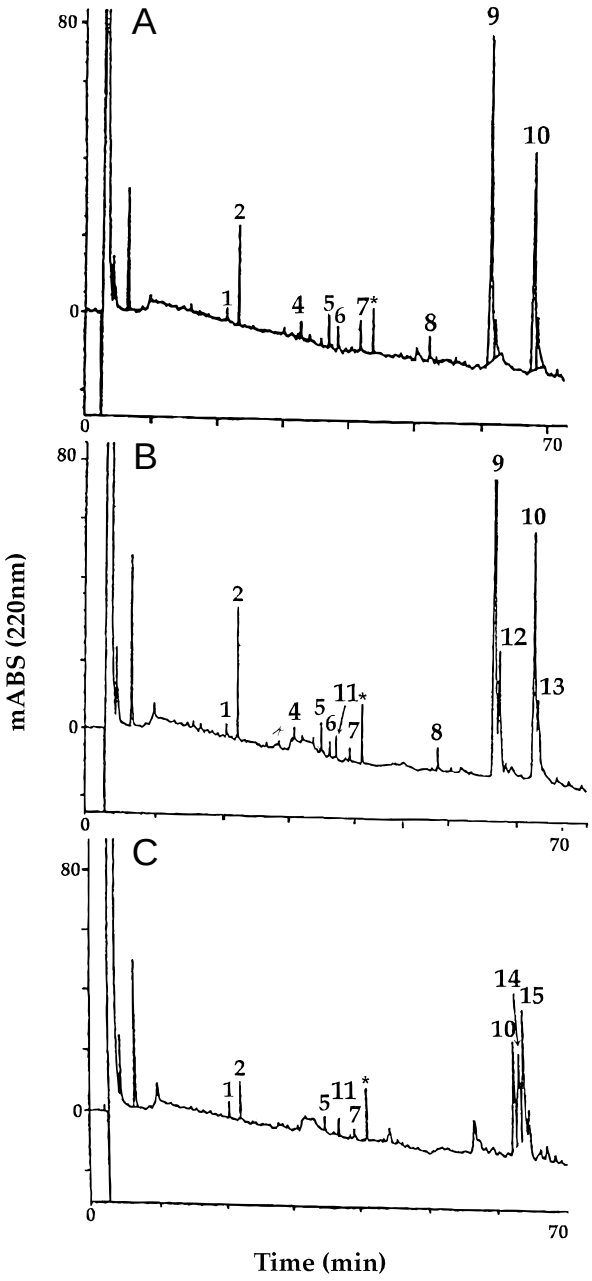

Fig. 4. HPLC analysis of $NS3_{1–180}$ digested with chymotrypsin under controlled conditions in the presence of (**A**) 10%, (**B**) 25%, and (**C**) 50% glycerol using enzyme:substrate ratios of 1:100, 1:85, and 1:25 (w/w), respectively. Individual fractions were collected and analyzed by ESMS. The CHAPS peak is marked with an asterisk.

However, several differences were detected when the proteolysis was performed at higher glycerol concentrations. At 25% glycerol (Fig. 4B), chymotrypsin digestion revealed the occurrence of a new cleavage site at Met180, as demonstrated by the presence of the fragments 8–180 and 23–180 (peaks 13 and 12 in Fig. 4B, respectively) not previously observed. A slightly susceptibility of Cys160 was detected due to the appearance of fraction 11 containing the peptide 161–180. The HPLC analysis showed the decrease of fractions 6 and 7 containing the peptides 156–187 and 136–155, thus suggesting a lower accessibility of Phe155.

A dramatic change in the HPLC profile was detected when the proteolysis was carried out at 50% glycerol. A remarkably large portion of intact $NS3_{1–180}$, remained undigested in these conditions (peak 14 in Fig. 4C), indicating a higher resistance to the proteolytic digestion possibly due to a more compact structure of the protein. Identification of the individual fractions demonstrated the increased accessibility of Met180 and the slower kinetic of hydrolysis at Tyr7 as shown by the appearance of peak 15, containing the fragment 3–180, and the concomitant decrease of fractions 2 and 10 (peptides 3–7 and 8–187, respectively). Moreover, Leu22 could barely be recognized by the protease, as shown by the almost complete disappearance of fragments 23–187 and 23–180, peaks 9 and 12 in Figure 4. Finally, it should be noted that proteolysis at Phe155 tended to be slower, as suggested by the disappearance of peak 6 and the further decrease of peak 7, indicating that under these conditions the active site of $NS3_{1–180}$ is more structured, and hence, less accessible.

These results clearly indicated that the overall structure of the NS3 protease was affected by increasing concentrations of glycerol. The protein adopted a more compact and rigid conformation, showing an increasing resistance to proteolytic cleavages. Conformational changes mainly occurred within the N-terminal tail that became less flexible and exposed, showing an almost complete protection of Leu22 and a much slower kinetics of hydrolysis at Tyr7. The C-terminal region was also affected, leading to the exposition of Met180. Finally, in the active site region of $NS3_{1–180}$, the accessibility of Phe155 decreased as the concentration of glycerol increased, with the concomitant exposure of Cys160.

Topological studies of the $NS3_{1–180}$/Pep4A complex

The experimental approach described above was employed to investigate the surface topology of the complex between the NS3 protease domain and an NS4A peptide following the strategy described previously (Scaloni et al., 1998). The complex was formed by incubating $NS3_{1–180}$ with a 10:1 molar excess of a 17-amino acid synthetic peptide encompassing the hydrophobic region of NS4A involved in the interaction with the viral protease, hereafter designed as Pep4A. Because this complex was stabilized in the presence of 50% glycerol (Bianchi et al., 1997), enzymatic digestions were all performed under these conditions using trypsin, chymotrypsin, and subtilisin as proteolytic probes. A 1:10 E/S ratio was used in all cases, as preliminary results had shown that the protein complex was resistant to proteolytic attack.

Figure 5 shows the HPLC time-course analysis of the complex digested with chymotrypsin. A number of fragments were released from unbound Pep4A due to the large excess of the cofactor peptide in solution. Control experiments performed using the peptide substrate Suc-Ala-Ala-Pro-Phe-4NA demonstrated that chymotrypsin activity was not affected by the presence of up to 300 μM of Pep4A. The chromatograms showed the occurrence of rapid cleavages at level of Tyr7 and Leu22, as revealed by the release of peptides 3–7, 23–187, and 8–187 after 15 min of enzymatic hydrolysis (peaks 2, 9, and 10 in Fig. 5A, respectively). As the hydrolysis time increased, species 23–187 became predominant, with the concomitant decrease of fragment 8–187. A further cleavage site was detected at Met180, originating fragment 23–180 (peak 12 in Fig. 5B). At later stages of incubation, a number of minor peaks could also be detected generated by hydrolysis occurring in the two inner protease-sensitive regions of $NS3_{1–180}$. Again, it should be noted that Phe155 and the adjacent Cys160 were recognized by chymotrypsin, as demonstrated by the presence of peptides 136–155 and 161–180 (peaks 7 and 11 in Fig. 5C, respectively).

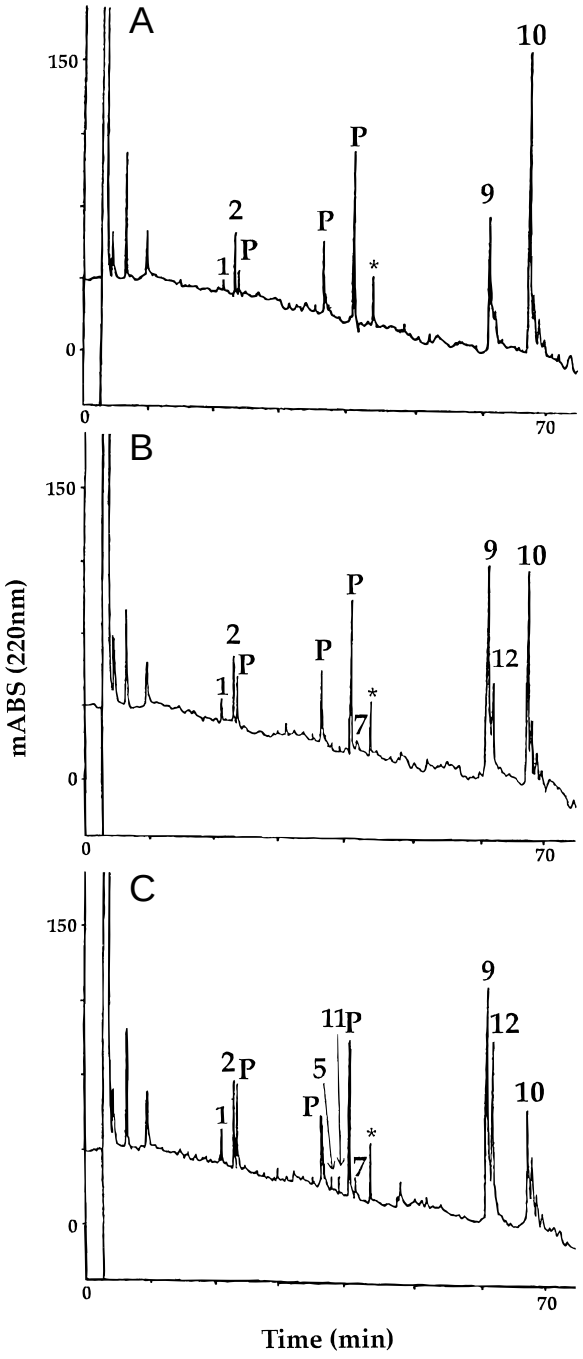

Fig. 5. Time-course analysis of the $NS3_{1–180}$/Pep4A complex digested with chymotrypsin under controlled conditions using an E/S ratio of 1:10. HPLC profiles of the aliquots withdrawn from the incubation mixture at (**A**) 15 min, (**B**) 30 min, and (**C**) 1 h. Individual fractions were collected and analyzed by ESMS. The CHAPS peak is marked with an asterisk; peaks marked with P correspond to digestion products of unbound Pep4A.

The overall results of the limited proteolysis investigation of the $NS3_{1–180}$/Pep4A complex are reported in Table 3. When these data were compared with those obtained on the isolated protease at 50% glycerol (Fig. 4C), a number of considerations could be drawn. The complex showed a lower accessibility to proteases than the isolated protein, as demonstrated by the higher E/S ratio needed to observe proteolytic cleavages, thus suggesting that the interaction with Pep4A led to a further increase in the compactness of the $NS3_{1–180}$ structure. Differences in the proteolytic sites were mainly located within the N-terminal arm, where a rapid hydrolysis at Tyr7 and Leu22 was observed. Chymotryptic digestion of isolated $NS3_{1–180}$ at 50% glycerol had shown slower kinetics of hydrolysis at Tyr7 and an almost completely shielding of Leu22 to proteolytic attack. These data suggested that following complex formation the N-terminal arm might adopt a different conformation compared to that observed at the same concentration of glycerol but in the absence of Pep4A. The C-terminal region seemed to be less affected by complex formation in that the accessibility of the preferential cleavage sites remained essentially unchanged, although a much slower hydrolysis at Met180 was observed. Finally, it should be mentioned that no changes in the hydrolysis at Phe155 and its neighboring residue Cys160 were observed, suggesting that the conformation of the NS3 active site was only slightly affected by the binding of the cofactor Pep4A.

Discussion

Conformational changes occurring within the tertiary structure of $NS3_{1–180}$ under different physico-chemical conditions either in the absence or in the presence of its cofactor Pep4A were probed by limited proteolysis combined with mass spectrometric methodologies. The overall strategy is based on the evidence that amino acid

Table 3. *Preferential cleavage sites detected on the $NS3_{1–180}$/Pep4A complex*[a]

Protease	Primary sites	Secondary sites	Protease-sensitive sites
Trypsin	Arg12	Arg25	
Chymotrypsin	Tyr7	Leu22	Trp86, Tyr106, Leu128, Tyr135, Phe155, Cys160, Met180
Subtilisin	Tyr7	Thr20	

[a]Different sites were classified as primary, secondary, and protease-sensitive merely on qualitative kinetic evaluation.

residues located within exposed and flexible regions of the protein can be recognized by proteases, leading to a reasonably good imprinting of the $NS3_{1–180}$ conformation in solution. Because the surface topology of the protein is affected by conformational changes, when comparative experiments were carried out on $NS3_{1–180}$ either at different glycerol concentrations or in the presence of Pep4A, differential peptide maps were obtained from which protein regions involved in the structural changes could be inferred.

As first stage, the surface topology of isolated $NS3_{1–180}$ in the presence of 10% glycerol was investigated, both as reference and to assess whether or not the crystal phase mimics the solution structure. Selective alkylation of the cysteine residues and limited proteolysis data were essentially consistent with the crystal structure of the protein determined by X-ray analysis (Love et al., 1996) and reported in Figure 6A, where the accessible sites are highlighted in red. For better clarity, the corresponding amino acid residues in the NS3 sequence are indicated in Figure 1. The surface topology of $NS3_{1–180}$ showed a characteristic pattern of exposed and buried regions. The N-terminal segment encompassing the first 25 residues was the most accessible portion where all the preferential proteolytic cleavages and the alkylated Cys17 were located, whereas protease-sensitive sites gathered into two inner regions, the fragments 65–86 and 124–179, the latter containing the other alkylated cysteine residue, Cys160. The pronounced accessibility of the extreme N-terminus is consistent with the presence of a long N-terminal strand, which extends away from the protein and is endowed with high conformational flexibility. In the crystal structure in the absence of the cofactor, the N-terminus interacts with neighboring molecules, through a strand swapping in which a hydrophobic patch on the surface of each molecule is bound to the N-terminal of a different neighbor (Love et al., 1996). These interactions are likely to be peculiar features of the crystallized enzyme, as the N-terminal segment showed accessibility at nearly all the possible sites, indicating that in solution this region is probably disordered.

Following alkylation of $NS3_{1–180}$ with iodoacetamide, a homogeneous doubly-derivatized species was obtained in which only Cys17 and Cys160 had been modified. This result is in contrast with previous data on selective chemical modifications of several other proteins that had always shown the formation of mixtures of isomeric components (Suckau et al., 1992; Glocker et al., 1994; Zappacosta et al., 1997; Scaloni et al., 1998) and supports the occurrence of a zinc binding site inferred by X-ray analysis (Love et al., 1996). This interaction coordinates the SH groups of Cys98, Cys100, and Cys146, and it is expected to reduce the chemical reactivity of these cysteines with respect to Cys17 and Cys160. The remaining Cys48 and Cys53 are buried inside the core of the protein and then could not be modified.

Our data confirm that the region containing the active site of NS3 has an open conformation, and it is endowed with considerable flexibility that can be correlated with an exceedingly low catalytic activity at 10% glycerol. In fact, glycerol has been shown to have dramatic effects on both enzyme activity, protein structure, and cofactor affinity (Steinkühler et al., 1996b; Bianchi et al., 1997). In line with these findings, a considerably different surface topology of $NS3_{1–180}$ was observed at higher glycerol concentrations as a consequence of conformational changes that mainly affected the extreme N- and C-terminal portions of the molecule. As a whole, the protein assumed a more compact structure showing a generally lower accessibility, possibly reflecting a gradual decrease in conformational flexibility with increasing concentrations of the cosolvent. A much slower kinetics of hydrolysis was observed at Tyr7, whereas Leu22 was not recognized by chymotrypsin, suggesting that this region became less exposed and flexible.

The enhancement of protein stability by cosolvents such as glycerol has been proposed to arise by "preferential hydration" of the protein, i.e., by exclusion of the cosolvent molecules from the surface–solvent interface (Timasheff, 1993). This exclusion is thermodynamically unfavorable, leading to a tendency of the system to decrease the protein–solvent contact area thereby, promoting protein compactness. Glycerol was also proposed to induce a release of "lubricant" water molecules, the presence of which maintains conformational flexibility by keeping apart adjacent segments of the polypeptide chain. This is expected to induce a collapse of the voids containing the water, thereby decreasing volume and compressibility of protein interior (Priev et al., 1996). In light of these effects, it may be argued that increasing concentrations of cosolvent might force the N-terminal segment to interact with exposed hydrophobic patches on the protein molecule with a concomitant decrease of conformational freedom. Alternatively, under these conditions, the hydrophobic regions occurring in the N-terminal tail might give rise to intermolecular interactions with neighboring molecules that mimic those observed in the crystal structure. Stabilization of dimeric structures by glycerol has recently been shown for other viral proteases (Cole, 1996; Darke et al., 1996; Margosiak et al., 1996).

At 50% glycerol the active site Phe155 also showed a reduced susceptibility toward chymotryptic action, suggesting that the con-

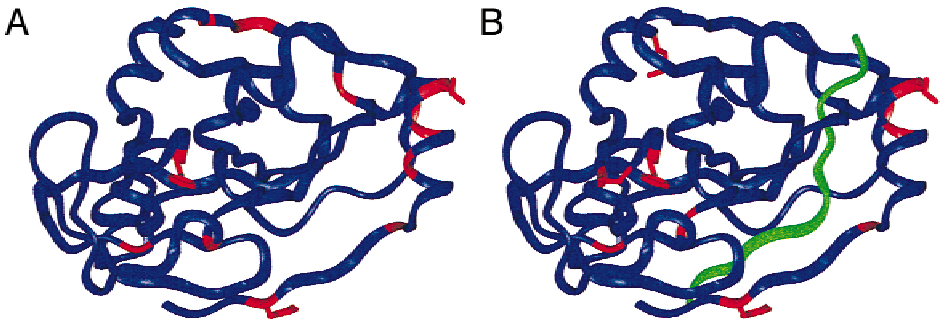

Fig. 6. Three-dimensional structure of isolated (**A**) $NS3_{1–180}$ and the (**B**) $NS3_{1–180}$/Pep4A complex. The backbone of Pep4A is in green; preferential cleavage sites are highlighted in red. The side chains of Tyr7, Leu22, and Phe155 are indicated in both panels, those of Cys160 and Met180 are displayed in **B**.

formational changes had caused the active site to adopt a more compact structure. Thus, the tightening of the region around the active site might account for the enhancement of the catalytic activity of $NS3_{1–180}$ observed at higher glycerol concentrations (Steinkühler et al., 1996b; Bianchi et al., 1997). In fact, only minor readjustments of the polypeptide chain would position the previously misaligned carboxylate of Asp82 closer to His58, as required for catalysis. It is, therefore, likely that the cosolvent has a pronounced effect especially on this region of the NS3 protease.

On the contrary, the structural changes occurring at the C-terminus of $NS3_{1–180}$ led to a higher exposure of the polypeptide chain that was rapidly cleaved at Met180. An increased accessibility of this region may be a direct consequence of an enhanced compactness of the segment 65–86, which is located in direct vicinity to the C-terminal helix. At low glycerol concentrations, the conformational mobility of this region may partially shield the underlying C-terminal helix from proteolytic attack, and a glycerol-induced tightening of the segment 65–86 may revert this situation.

Further conformational changes were detected in the surface topology of $NS3_{1–180}$ when proteolytic experiments were carried out in the presence of the cofactor Pep4A (Fig. 6B). Following complex formation, the N-terminal portion of the protease again became highly susceptible to proteolytic enzymes, with a number of residues located in the segment 7–25 rapidly cleaved by proteases. These data suggest that in solution the N-terminal arm is displaced from the protein moiety by the interaction with the cofactor peptide, again becoming exposed to proteolytic attack. X-ray crystallography data showed a very tight interaction between $NS3_{1–180}$ and the cofactor, with Pep4A being an integral part of the N-terminal region of $NS3_{1–180}$. Such a complex is expected to be very stable, much tighter than the previously determined micromolar equilibrium dissociation constants. Limited proteolysis results then support thermodynamic data in that the N-terminus of $NS3_{1–180}$ seem to only marginally contribute to the stability of the complex (C. Steinkühler, pers. obs.).

The pattern of preferential proteolytic sites in the complex is resembling that found in the isolated protease at 10% glycerol and is in agreement with the structure of one of the complexes described by Kim et al. (1996) in which the N-terminal tail has a disordered and flexible conformation. This view supports previous hypotheses based on comparative spectroscopic studies that the N-terminus of $NS3_{1–180}$ exhibits the same secondary structure both in the complex and in the isolated molecule, but it is endowed with higher conformational freedom in the absence of Pep4A (Bianchi et al., 1997). Moreover, the displacement of the N-terminal tail needed to accommodate the cofactor peptide might constitute the rate-limiting step in the association of Pep4A, thus explaining the slow on-rate of complex formation (Bianchi et al., 1997). The observed conformational changes might be directly related to the mechanism of activation of the protease by its cofactor peptide. The tightening of the N-terminal domain due to the binding of the Pep4A, in fact, could be instrumental to a correct alignment of the catalytic triad, as discussed above, thus explaining the concomitant increase in k_{cat} values (Bianchi et al., 1997; Urbani et al., 1997; Yan et al., 1998).

Altogether, these data suggest that the NS3 protease domain has a high conformational flexibility, especially affecting the extreme N-terminus of the molecule, that may serve a specific physiological role. In fact, cleavage between NS2 and NS3, generating the mature N-terminus of the NS3 protein, is accomplished intramolecularly by a so far poorly characterized protease. At this stage of the processing cascade, the N-terminus of NS3 must adopt a conformation that allows the intramolecular cleavage to occur. Once the mature N-terminus of NS3 has been generated, it is believed to engage in an interaction with NS4A that leads to the activation of the NS3 protease. Again, the N-terminus of NS3 will have to adopt a conformation that allows complex formation with the cofactor. The observed conformational flexibility may account for the different roles performed by the N-terminal domain of NS3 during the processing and complexation events in which it is involved. The stabilizing properties of glycerol in vitro may simply indicate that other factors concur to stabilize the complex in vivo, such as membranes, the N-terminus of NS4A, which is believed to form a *trans*-membrane helix, thereby anchoring the NS3/NS4A complex to the ER, or the C-terminus of the NS3 protein, harboring the helicase domain. More studies will have to be performed with full-length proteins to shed light on the molecular details of the function of this key player in the viral life cycle.

Materials and methods

Trypsin TPCK-treated, chymotrypsin, subtilisin, and proteinase K were purchased from Sigma (St. Louis, Missouri); iodoacetamide was from Fluka (Buchs, Switzerland); Suc-Ala-Ala-Pro-Phe-4-NA synthetic peptide was from Calbiochem (La Jolla, California). RP-HPLC columns C4 and C18 (25 × 0.46 cm, 5 mm) were purchased from Vydac (The Separation Groups, Hesperia, California); prepacked PD10 Sephadex G-25 columns were from Pharmacia (Uppsala, Sweden). All other reagents and solvents were HPLC-grade from Carlo Erba (Milano, Italy).

Characterization of $NS3_{1–180}$

The protease domain of the HCV Bk strain NS3 protein encompassing residues 1027–1206 of the viral polyprotein, containing a C-terminal fusion with the sequence ASKKKK, was purified from *E. coli*, as previously described (Urbani et al., 1997). The homogeneity of the $NS3_{1–180}$ preparation was verified by analyzing a 1 nmol aliquot of the protein by a RP-HPLC C4 column. The protease was eluted by means of a linear gradient from 20 to 65% of acetonitrile in 0.1% TFA over 33 min; elution was monitored at 220 and 280 nm. Individual fractions were collected and identified by ESMS.

Chemical modification experiments

Modification of cysteine residues in $NS3_{1–180}$ was carried out by incubating 37 μg of the protein with iodoacetamide in 100 μL final volume using a reagent to a total thiol groups ratio of 0.9:1. The reaction was performed in 50 mM sodium phosphate buffer pH 7.5, containing 10% glycerol, 5 mM DTT, and 0.05% CHAPS, at 25 °C, in the dark, under nitrogen atmosphere for 15 min. The extent of protein modification was tested by HPLC analysis of an aliquot of the incubation mixture using a Vydac C4 column; the differently modified species of $NS3_{1–180}$ were eluted by means of the gradient previously described and the individual fractions were collected and analyzed by ESMS. When the desired number of modified cysteines was obtained, the remaining portion of the incubation mixture was desalted by gel filtration chromatography on a PD10 prepacked column, eluted with 50 mM sodium phosphate buffer (pH 7.5) containing 10% glycerol, 0.5 mM DTT, and 0.05% CHAPS. The eluted protein was then digested with trypsin

at 25 °C for 3 h using a 1:50 (w/w) enzyme:substrate ratio, and the resulting peptide mixture was fractionated by RP-HPLC on a Vydac C18 column.

Limited proteolysis experiments

Limited proteolysis experiments were carried out by incubating $NS3_{1–180}$ with trypsin, chymotrypsin, subtilisin, and proteinase K. Enzymatic digestions were all performed in 50 mM sodium phosphate (pH 7.5) containing 10% glycerol, 2.5 mM DTT, and 0.5% CHAPS, at 25 °C and using a 1:100 or 1:500 (w/w) enzyme-to-substrate ratio. The extent of the reaction was monitored on a time-course basis by sampling the incubation mixture at different times intervals. Proteolytic fragments were fractionated by RP-HPLC on a Vydac C18 column, and the individual fractions were manually collected and analyzed by ESMS. Chymotryptic digestions at different concentrations of glycerol were carried out under the same conditions in the presence of 10, 25, and 50% glycerol using enzyme:substrate ratios of 1:100, 1:85, and 1:25 (w/w), respectively.

When the experiments were performed on the $NS3_{1–180}$/Pep4A complex, $NS3_{1–180}$ was pre-incubated with a 10:1 excess of Pep4A, encompassing residues 21–34 of the NS4A protein together with an N-terminal lysine tag (Bianchi et al., 1997), in 50 mM sodium phosphate, pH 7.5, containing 50% glycerol, at 25 °C for 10 min prior to the protease addiction. Digestions were performed using a 1:15 enzyme:substrate ratio.

Chromatographic separation of peptides

Peptide mixtures from the different proteolysis experiments were fractionated by RP-HPLC on a Vydac C18 column. Peptides were eluted by means of a linear gradient from 5 to 65% of acetonitrile in 0.1% TFA over 73 min; elution was monitored at 220 and 280 nm. Fractions were collected and identified by ESMS.

Mass spectrometry

Protein samples and proteolytic fragments were analyzed by ESMS using a Bio-Q triple quadrupole mass spectrometer (Micromass, Manchester, United Kingdom) equipped with an electrospray ion source. Samples were injected into the ion source (kept at 80 °C) via a loop injection at a flow rate of 10 μL/min. Data were acquired and elaborated using the MASSLYNX program, purchased from Micromass. Mass calibration was performed by means of multiply charged ions from a separate injection of horse heart myoglobin (Sigma; average molecular mass: 16,951.5 Da); all masses are reported as average values.

Acknowledgments

The authors wish to thank Dr. Antonello Pessi for helpful discussions and Dr. Anna Tramontano for providing Figure 6. This work was supported in part by MURST, Progetto di Ricerca di Interesse Nazionale (PRIN) “Biologia Strutturale.”

References

Bartenschlager R, Ahlborn-Laake L, Mous J, Jacobsen H. 1993. Nonstructural protein 3 of the Hepatitis C Virus encodes a serine-type proteinase required for cleavage at the NS3/4 and NS4/5 junctions. *J Virol 67*:3835–3844.

Bartenschlager R, Lohmann V, Wilkinson T, Koc JA. 1995. Complex formation between the NS3 serine-type proteinase of the Hepatitis C Virus and NS4A and its importance for polyprotein maturation. *J Virol 69*:7519–7528.

Bianchi E, Urbani A, Biasiol G, Brunetti M, Pessi A, De Francesco R, Steinkühler C. 1997. Complex formation between the Hepatitis C Virus serine protease and a synthetic NS4A cofactor peptide. *Biochemistry 36*:7890–7897.

Butkiewicz N, Wende M, Zhang R, Jubin R, Pichardo J, Smith E, Hart A, Ingram R, Durkin J, Mui P, et al. 1996. Enhancement of Hepatitis C Virus NS3 proteinase activity by association with NS4A specific synthetic peptides: Identification of the sequence and critical residues of NS4A for the cofactor activity. *Virology 225*:328–338.

Choo Q-L, Richman KH, Han HJ, Berger K, Lee C, Dong C, Colt D, Medina-Selby R, Barr PJ, Weiner AJ, et al. 1991. Genetic organization and diversity of the hepatitis C virus. *Proc Natl Acad Sci USA 88*:2451–2455.

Cohen SL, Ferrè-D'Amarè AR, Burley KS, Chait BT. 1995. Probing the solution structure of the DNA-binding protein Max by a combination of proteolysis and mass spectrometry. *Protein Sci 4*:82–87.

Cole J. 1996. Characterization of human Cytomegalovirus protease dimerization by analytical centrifugation. *Biochemistry 35*:15601–15610.

Darke PL, Cole JL, Waxman L, Hall DL, Sardana M, Kuo LC. 1996. Active human Cytomegalovirus protease is a dimer. *J Biol Chem 271*:7445–7449.

Eckart MR, Selby M, Masiarz F, Lee C, Berger K, Crawford K, Kuo C, Kuo G, Houghton M, Choo Q-L. 1993. The Hepatitis C Virus encodes a serine protease involved in the processing of the putative nonstructural proteins from the viral polyprotein precursor. *Biochem Biophys Res Commun 192*:399–406.

Failla C, Tomei L, De Francesco R. 1994. Both NS3 and NS4A are required for the proteolytic processing of Hepatitis C Virus nonstructural proteins. *J Virol 68*:3753–3760.

Failla C, Tomei L, De Francesco R. 1995. An amino-terminal domain of Hepatitis C Virus NS3 protease is essential for interaction with NS4A. *J Virol 69*:1769–1777.

Glocker MO, Bacher C, Fielder W, Suckau D, Przybylski K. 1994. Molecular characterisation of surface topology in protein tertiary structures by amino-acylation and mass spectrometric peptide mapping. *Bioconj Chem 5*:583–590.

Grakoui A, McCourt DW, Wychowski C, Feinstone SM, Rice CM. 1993. Characterisation of the Hepatitis C Virus-encoded serine proteinase: Determination of proteinase-dependent polyprotein cleavage sites. *J Virol 67*:2832–2843.

Hijikata M, Mizushima H, Akagi T, Mori S, Kakiuchi N, Kato N, Tanaka T, Kimura K, Shimotohno K. 1993. Two distinct proteinase activities required for the processing of a putative nonstructural precursor protein of Hepatitis C Virus. *J Virol 67*:4665–4675.

Houghton M, Weiner A, Han J, Kuo G, Choo Q-L. 1991. Molecular biology of the Hepatitis C Viruses: Implications for diagnosis, development and control of viral disease. *Hepatology 14*:381–388.

Kato N, Hijikata M, Oostuyama Y, Nagawaka M, Ohkoshi S, Sugimura T, Shimotohno K. 1990. Molecular cloning of the human Hepatitis C Virus genome from Japanese patients with non-A, non-B hepatitis. *Proc Natl Acad Sci USA 87*:9524–9528.

Kim JL, Morgenstern KA, Lin C, Fox T, Dwyer MD, Landro JA, Chambers SP, Markland W, Lepre CA, O'Malley ET, et al. 1996. Crystal structure of the Hepatitis C Virus NS3 protease domain complexed with a synthetic NS4A cofactor peptide. *Cell 87*:343–355.

Koch JO, Lohmann V, Herian U, Bartenschlager R. 1996. *In vitro* studies on the activation of the Hepatitis C Virus NS3 protease by the NS4A cofactor. *Virology 221*:54–66

Komoda Y, Hijikata M, Tanji Y, Hirowatari Y, Mizushima H, Kimura K, Shimotohono K. 1994. Processing of Hepatitis C viral polyprotein in *Escherichia coli*. *Gene 145*:221–226.

Lin C, Pragai BM, Grakoui A, Xu J, Rice CM. 1994. Hepatitis C Virus NS3 serine proteinase: *Trans*-cleavage requirements and processing kinetics. *J Virol 68*:8147–8157.

Lin C, Thomson JA, Rice CM. 1995. A central region in the Hepatitis C Virus NS4A protein allows formation of an active NS3–NS4A serine proteinase complex *in vivo* and *in vitro*. *J Virol 69*:4373–4380.

Love RA, Parge HE, Wickersham JA, Hostomsky Z, Habuka N, Moomaw EW, Adachi T, Hostomska Z. 1996. The crystal structure of Hepatitis C Virus NS3 proteinase reveals a trysin-like fold and a structural zinc binding site. *Cell 87*:331–342.

Margosiak SA, Vanderpool DL, Sisson W, Pinko C, Kan CC. 1996. Dimerization of the human Cytomegalovirus protease: Kinetic and biochemical characterisation of the catalytic homodimer. *Biochemistry 35*:5300–5307.

Mori A, Yamada J, Kimura T, Koide T, Yuasa S, Yamada E, Miyamura T. 1996. Enzymatic characterisation of purified NS3 serine proteinase of Hepatitis C Virus expressed in *Escherichia coli*. *FEBS Lett 378*:37–42.

Pizzi E, Tramontano A, Tomei L, La Monica N, Failla C, Sardana M, Wood T,

De Francesco R. 1994. Molecular modelling of the specificity pocket of the Hepatitis C Virus protease: Implications for substrate recognition. *Proc Natl Acad Sci USA 91*:888–892.

Priev A, Almagor A, Yedgar S, Gavish B. 1996. Glycerol decreases the volume and compressibility of protein interior. *Biochemistry 35*:2061–2066.

Satoh S, Tanji Y, Hijikata M, Kimura K, Shimotohno K. 1995. The N-terminal region of Hepatitis C Virus nonstructural protein 3 (NS3) is essential for stable complex formation with NS4A. *J Virol 69*:4255–4260.

Scaloni A, Miraglia N, Orrù S, Amodeo P, Motta A, Marino G, Pucci P. 1998. Topology of Calmodulin–Melittin complex. *J Mol Biol 277*:945–958.

Shoji I, Suzuki T, Chieda S, Sato M, Harada T, Chiba T, Matsuura Y, Miyamura T. 1995. Proteolytic activity of NS3 serine proteinase of Hepatitis C Virus efficiently expressed in *Escherichia coli*. *Hepatology 22*:1648–1655.

Steinkühler C, Biasiol G, Brunetti M, Urbani A, Koch U, Cortese R, Pessi A, De Francesco R. 1998. Product inhibition of the Hepatitis C Virus NS3 protease. *Biochemistry 37*:8899–8905.

Steinkühler C, Tomei L, De Francesco R. 1996a. *In vitro* activity of Hepatitis C Virus protease NS3 purified from recombinant baculovirus-infected Sf9 cells. *J Biol Chem 271*:6367–6373.

Steinkühler C, Urbani A, Tomei L, Sardana M, Bianchi E, Pessi A, De Francesco R. 1996b. Activity of purified Hepatitis C Virus protease NS3 on peptide substrates. *J Virol 70*:6694–6700.

Suckau D, Mark M, Przybylski M. 1992. Protein surface topology-probing by selective chemical modification and mass spectrometric peptide mapping. *Proc Natl Acad Sci USA 89*:5630–5634.

Suzuki T, Sato M, Chieda S, Shoji I, Harada T, Yamakawa Y, Watabe S, Matsuura Y, Miyamura T. 1995. *In vivo* and *in vitro* trans-cleavage activity of Hepatitis C Virus serine proteinase expressed by recombinant baculoviruses. *J Gen Virol 76*:3021–3029.

Takamizawa A, Mori C, Fuke I, Manabe S, Murakame S, Fujita J, Onoshi E, Andoh T, Yoshida Y, Okayama H. 1991. Structure and organisation of the Hepatitis C Virus genome isolated from human carriers. *J Virol 65*:1105–1113.

Tanji Y, Hijikata M, Hirowatari Y, Shimotohno K. 1995. Hepatitis C virus-encoded nonstructural protein NS4A has versatile functions in viral protein processing. *J Virol 69*:1575–1581.

Timasheff SN. 1993. The control of protein stability and association by weak interaction with water: How do solvents affect these processes. *Annu Rev Biophys Biomol Struct 22*:67–97.

Tomei L, Failla C, Santolini E, De Francesco R, La Monica N. 1993. NS3 is a serine protease required for processing of Hepatitis C Virus polyprotein. *J Virol 67*:4017–4026.

Tomei L, Failla C, Vitale RL, Bianchi E, De Francesco R. 1996. A central hydrophobic domain of the Hepatitis C Virus NS4A protein is required and sufficient for the activation of the NS3 protease. *J Gen Virol 77*:1065–1070.

Urbani A, Bianchi E, Narjes F, Tramontano A, De Francesco R, Steinkühler C, Pessi A. 1997. Substrate specificity of the Hepatitis C Virus serine protease NS3. *J Biol Chem 272*:9204–9209.

Yan Y, Li Y, Sardana V, Cole JL, Sardana M, Steinkühler C, Tomei L, De Francesco R, Kuo LC, Chen Z. 1998. Complex of NS3 protease and NS4A peptide of BK strain Hepatitis C Virus: A 2.2 Å resolution structure in a hexagonal crystal form. *Protein Sci 7*:837–847.

Zappacosta F, Ingallinella P, Scaloni A, Pessi A, Bianchi E, Sollazzo M, Tramontano A, Marino G, Pucci P. 1997. Surface topology of Minibody by selective chemical modification and mass spectrometry. *Protein Sci 6*:1901–1909.

Zappacosta F, Pessi A, Bianchi E, Venturini S, Sollazzo M, Tramontano A, Marino G, Pucci P. 1996. Probing the tertiary structure of proteins by limited proteolysis and mass spectrometry: The case of Miniboby. *Protein Sci 5*:802–813.